



Published in final edited form as:

Acta Biomater. 2022 October 01; 151: 278–289. doi:10.1016/j.actbio.2022.08.010.

Charge-based drug delivery to cartilage: Hydrophobic and not electrostatic interactions are the dominant cause of competitive binding of cationic carriers in synovial fluid

Armin Vedadghavami^a, Tengfei He^a, Chenzhen Zhang^a, Salima M. Amiji^a, Bill Hakim^a, Ambika G. Bajpayee^{a,b,*}

^aDepartment of Bioengineering, Northeastern University, Boston, MA 02115, USA

^bDepartment of Mechanical Engineering, Northeastern University, Boston, MA 02115, USA

Abstract

Charge-based drug delivery has proven to be effective for targeting negatively charged cartilage for the treatment of osteoarthritis. Cartilage is surrounded by synovial fluid (SF), which is comprised of negatively charged hyaluronic acid and hydrophobic proteins that can competitively bind cationic carriers and prevent their transport into cartilage. Here we investigate the relative contributions of charge and hydrophobic effects on the binding of cationic carriers within healthy and arthritic SF by comparing the transport of arginine-rich cartilage targeting cationic peptide carriers with hydrophilic (CPC +14N) or hydrophobic property (CPC +14A). CPC +14N had significantly greater intra-cartilage uptake in presence of SF compared to CPC +14A *in-vitro* and *in vivo*. In presence of individual anionic SF constituents, both CPCs maintained similar high intra-cartilage uptake while in presence of hydrophobic constituents, CPC +14N had greater uptake confirming that hydrophobic and not charge interactions are the dominant cause of competitive binding within SF. Results also demonstrate that short-range effects can synergistically stabilize intra-cartilage charge-based binding – a property that can be utilized for enhancing drug-carrier residence time in arthritic cartilage with diminished negative fixed charge density. The work provides a framework for the rational design of cationic carriers for developing targeted therapies for another complex negatively charged environments.

Statement of significance—This work demonstrates that hydrophobic and not charge interactions are the dominant cause of the binding of cationic carriers in synovial fluid. Therefore, cationic carriers can be effectively used for cartilage targeting if they are made hydrophilic. This can facilitate clinical translation of various osteoarthritis drugs for cartilage repair that have failed due to a lack of effective cartilage targeting methods. It also demonstrates that short-range hydrogen bonds can synergistically stabilize electrostatic binding in cartilage offering a method for enhancing the targeting and residence time of cationic carriers within arthritic cartilage with reduced charge density. Finally, the cartilage-synovial fluid unit provides an excellent model of a

*Corresponding author at: Department of Bioengineering, Northeastern University, ISEC Room 216, 805 Columbus Avenue, Boston, MA 02115, USA. a.bajpayee@northeastern.edu (A.G. Bajpayee).

Declaration of Competing Interest

The authors declare no conflict of interests.

The authors declare that they have no known competing financial interests or personal relationships that could have appeared to influence the work reported in this paper.

complex negatively charged environment and allows us to generalize these findings and develop targeted therapies for other charged tissue-systems.

Keywords

Charge interactions; Hydrophobic interactions; Cartilage; Fixed charge density; Drug delivery; Synovial fluid

1. Introduction

Charge-based drug delivery has proven to be an effective way of targeting negatively charged tissues like cartilage for the treatment of osteoarthritis (OA), which is a degenerative musculoskeletal disease [1–4]. Cartilage has a high negative fixed charge density (FCD ~ -170 mM) owing to the presence of densely packed negatively charged aggrecan glycosaminoglycans (GAGs) that are key to the tissue's structure and function as they provide the necessary hydration, swelling pressure, and compressive stiffness [3]. Cartilage is also avascular and thus direct injections into the intra-articular (IA) space of joints are used for delivering drugs. However, transport of most macromolecules into cartilage is hindered due to its dense extracellular matrix with a nanometer range pore size [5]. Cartilage is surrounded by synovial fluid (SF) and relies on passive diffusion of compression induced (due to joint movement) convective diffusion to transport drugs from SF into cartilage to reach their cell targets [6,7]. The SF is under constant turnover due to clearance from the lymphatics and synovium vasculature resulting in a very short (1-2 h) intra-joint residence time for small molecules [5]. As such, drugs rapidly clear out from the joint before the required intra-cartilage therapeutic index can be achieved [8]. Multiple injections of high drug doses may be indicated which are associated with toxicity concerns [9].

This high negative FCD of cartilage (and other tissues) can be converted from being a challenge to an opportunity by modifying therapeutics to add optimally charged cationic domains such that electrostatic interactions can be used for enhancing their intra-tissue uptake and retention [10–17]. Our previous studies have demonstrated that the design of cationic carriers can be optimized based on the target tissue FCD to possess enough electrical driving force to rapidly penetrate through the tissue's full thickness in high concentrations to reach their cell targets [1,2]. We designed an arginine-rich cationic peptide carrier (CPC) with a net charge of +14 and demonstrated a very high intra-cartilage uptake of 350 (i.e., a solute concentration inside cartilage was 350x higher than the surrounding bath [1]. Note that an uncharged small molecule will have an equilibrium uptake of 1). CPC +14's intra-cartilage uptake was the highest among other CPCs with lower or higher net charge (the net charge was varied between +8 and +20). CPC +14 measured a high Donnan partitioning factor of 3.4 that facilitated its rapid penetration through the full thickness of cartilage owing to the weak-reversible nature of charge interactions. Despite this weak binding, the high density of intra-cartilage negatively charged GAG binding sites enabled its long-term retention as >95% of CPC +14 was found to be retained within cartilage over 7-days desorption period, which was the longest duration over which the experiment was conducted [1].

SF is another barrier for targeted drug delivery to cartilage; its interactions with carriers should be taken into account while designing drug delivery systems but are often overlooked [18]. SF is an ultrafiltrate of blood plasma through the synovial membrane and is comprised of negatively charged hyaluronic acid (HA), a non-sulfated GAG chain secreted by the synoviocytes primarily responsible for providing joint lubrication [19]. HA is present at a concentration of 1–3 mg/ml conferring it an FCD of –8.8 mM [3]. SF is also comprised of high levels of plasma proteins, mainly anionic albumin (~ 12 mg/ml) and hydrophobic globulin (β_1 , γ , α_1 , and α_2 each at 1–3 mg/ml), and a low concentration of hydrophobic phospholipids (Fig. 1, Table 1) [20]. Therefore, competing bindings effects from charge and hydrophobic interactions are expected within SF, which can hinder electro-diffusive transport and cartilage targeting properties of cationic carriers. Additionally, the HA content and viscosity of SF decrease with arthritis severity [21]. It is also associated with an increase in degraded GAGs that diffuse out from cartilage, which may also compete with cationic carriers' diffusion into cartilage.

2. Materials and methods

2.1. Materials

Protease Inhibitor Mini Tablets were purchased from Thermo Scientific Pierce (Rockford, IL). Penicillin-streptomycin Antibiotic-Antimycotic (PSA) and trypsin-EDTA phenol red were purchased from Gibco (Carlsbad, CA). Tween-20, glycerol, sodium chloride (NaCl), and bovine serum albumin (BSA) were obtained from Fisher Bioreagents (Fair Lawn, NJ). Trizma base, Chondroitin sulfate (CS), hyaluronic acid (HA), and Sodium dodecyl sulfate (SDS) were from Sigma-Aldrich (St. Louis, MO). 2-Dilauroyl-sn-glycero-3-phosphocholine (DLPC) was purchased from Echelon Biosciences (Salt Lake City, UT). Gamma globulin (γ -Globulin) from bovine serum was procured from EMD Millipore (Billerica, MA). Proteinase-K was purchased from Roche Diagnostics (Risch-Rotkreuz, Switzerland).

2.2. Design and synthesis of Cationic Peptide Carriers (CPC)

20 amino acid-long Cationic Peptide Carriers (CPCs) with a net charge of +14, rich in cationic arginine (R) and non-polar alanine (A) or polar asparagine (N) residues as spacers were synthesized using Fmoc solid-phase peptide synthesis (MIT Biopolymers and Proteomics, MIT, Cambridge, MA). The hydrophobic version with alanine spacers is referred to as **CPC +14A** and the hydrophilic version with asparagine is referred to as **CPC +14N** (Table 2). A sequence with no spacers (A or N) is used as a control (**R+14**) with similar net charge and hydrophilic property. In addition to these, to evaluate the effect of reducing the net charge and increasing the relative hydrophobicity on electro-diffusive transport of CPCs in cartilage in presence of synovial fluid, an R-rich CPC with a net charge of +8 (**CPC +8A**) was included. Finally, to study the competitive effects of charge and hydrophobicity, a charge dominant lysine (K) – rich CPC with net charge +7 (**AK**)₇ was used with either a hydrophilic tail (ANANAN, asparagine spaced with alanine; **CPC +N**) or a hydrophobic tail (AFAFAF, phenylalanine with alanine; **CPC +F**). Table 3 shows the hydropathy scale of different amino acids [22]. The peptides were purified using reverse phase C18 HPLC (resulting in >95% purity) and CPC masses were confirmed by matrix-assisted laser desorption/ionization (MALDI) mass spectrometry. For fluorescence

measurements, CPCs were either labeled with 5-FAM for *in-vitro* studies or Cy5 for *in vivo* experiments.

2.3. Intra-cartilage transport of CPCs in presence of synovial fluid and its individual constituents

2.3.1. Cartilage explant harvest—Full-thickness 3 mm diameter cartilage plugs were extracted from 2–3 week-old bovine knee joints purchased from a local slaughterhouse (Research 87, Boylston, MA). The plugs were then sliced to obtain 1 mm thick cartilage disks from the superficial layer as described before [15]. The disks were immediately washed and equilibrated in PBS supplemented with PSA for 1 h and stored in PBS supplemented with protease inhibitors at -20°C until further use. Late-stage OA explants were prepared by explants incubation in 0.1 mg/ml of trypsin-EDTA phenol red in PBS for 14 h to induce $\sim 90\%$ GAG depletion. The explants were washed three times in PBS and equilibrated for an hour in PBS supplemented with protease inhibitors to arrest the digestion. GAG depletion percentage was measured using dimethyl-methylene blue (DMMB) assay [23].

2.3.2. Healthy and arthritic synovial fluid (SF)—Simulated SF was constituted using 3 mg/ml HA (MW ~ 1.5 MDa), 12 mg/ml BSA, 12 mg/ml γ -Globulin and 0.1 mg/ml DLPC in PBS at pH 7.4 based on physiological concentrations of individual SF constituents (Table 1) and previous work [24,25]. Experiments were conducted in simulated SF to provide a controlled healthy environment for comparison is referred as **Healthy SF**. Bovine synovial fluid (SF) from Lampire Biological Laboratories (Pipersville, PA) was aliquoted and frozen at -20°C until the day of the experiment – this is referred as **OA SF**. The content of sulfated glycosaminoglycans (GAGs) in bovine SF was measured using DMMB assay [26] to quantify and determine the severity of OA.

2.3.3. Equilibrium uptake of CPCs in bovine cartilage—To study the equilibrium uptake of CPCs in cartilage in presence of SF, 30 μM CPC solution was made in either Healthy or OA SF. Individual 3×1 mm cartilage disks were equilibrated in 300 μl of 30 μM CPC solution in a 96 well plate for 24 h at 37°C under gentle shaking in an incubator [27]. The fluorescence of the initial and final equilibration CPC baths was measured using a microplate reader (Synergy H1, Biotek) and converted to CPC concentration using a standard curve as described before [1]. The uptake ratio (R_U , Eq. (1)) was defined as the CPC concentration inside cartilage ($\bar{C}_{cartilage}$) normalized by the CPC concentration in the surrounding SF bath at equilibration (C_{Bath}):

$$R_U = \frac{\bar{C}_{cartilage}}{C_{Bath}}; \quad (1)$$

To determine the effects of SF constituents on intra-cartilage uptake of CPCs, experiments were conducted in presence of individual SF constituents at their physiological concentrations, i.e., either 3 mg/ml HA, 12 mg/ml BSA, 12 mg/ml γ -Globulin, or 0.1 mg/ml DLPC, which was used as a model for phospholipids.

2.3.4. The binding affinity of CPCs with SF and cartilage matrix constituents

—The binding affinity of CPCs with individual SF and cartilage constituents was determined using microscale thermophoresis (MST, Monolith NT.115, NanoTemper Technologies, Munich, Germany) [28]. The stock solutions of CPCs labeled with 5-FAM at the N-terminus were centrifuged at 14,000 g for 10 min prior to the experiment to remove any aggregates. Binding interactions were measured in a buffer consisting of 50 mM Tris pH 7.4, 150 mM NaCl, 0.005% SDS, 0.1% Tween-20 and 0.025% glycerol. These buffer conditions were optimized to minimize CPC binding with the capillaries while ensuring that MST trace curves can achieve fluorescence equilibrium. 200 nM of fluorescently labeled CPCs were used as target molecules and titrated individually with serial dilutions of CS, HA, and γ -Globulin as the ligand molecules. The samples were then loaded on Monolith Premium capillaries and MST measurements were carried out under 50% excitation power and 40% MST power at room temperature (Fig. 2A). Briefly, each sample was locally heated using the IR-Laser and the fluorescence values were normalized by the initial fluorescence prior to heating of the sample ($F_{Norm}(\%)$) were plotted against time to obtain an MST trace curve (Fig. 2B, C). Laser on and off times was set as 20 s and 5 s, respectively. The normalized fluorescence at 5 s from the MST traces of all samples was chosen to plot the binding curve (Fig. 2C, D). The $F_{Norm}(\%)$ of each sample was subtracted from the baseline $F_{Norm}(\%)$ at the completely unbound state to produce $\Delta F_{Norm}(\%)$ values (Eq. (2)).

$$\Delta F_{Norm}(\%) = \frac{F_{Norm}(C_{Ligand}) - F_{Norm}(unbound)}{F_{Norm}(bound) - F_{Norm}(unbound)}; \quad (2)$$

Where $F_{Norm}(C_{Ligand})$ is the normalized fluorescence at a given ligand concentration, $F_{Norm}(unbound)$ is the normalized fluorescence of only unbound CPC and $F_{Norm}(bound)$ is the normalized fluorescence of CPC when completely bound by the ligand. Hill equation was fitted to all the binding curves consisting of $\Delta F_{Norm}(\%)$ values versus ligand concentrations using the MO Affinity Analysis software (Eq. (3), Fig. 2D) to determine the dissociation constant (K_d) and Hill coefficient co-operativity factor (n):

$$\Delta F_{Norm}(\%) = \frac{F_{Norm}(C_{Ligand}) - F_{Norm}(unbound)}{F_{Norm}(bound) - F_{Norm}(unbound)} = \frac{1}{1 + \left(\frac{K_d}{C_{Ligand}}\right)^n}; \quad (3)$$

Hill coefficient (n) represents the degree of co-operativity in the binding event. A coefficient of $n > 1$ represents positive cooperativity, in which the binding of one molecule facilitates the binding of subsequent molecules to its binding partner. A coefficient of $n < 1$ represents negative cooperativity, meaning the binding of one molecule makes it difficult for subsequent molecules to bind [29].

2.4. In vivo biodistribution of CPCs in rat knee joint

Animal studies were performed and pre-approved by the Institutional Animal Care and Use Committee at Northeastern University. Injections of 50 μ l of 300 μ M CPC +14A or CPC +14N labeled with Cy5 dye were administered intra-articularly through the patellar tendon into the knee joints of healthy 8–10-week-old male Wistar rats weighing between 350 and

400 g (Charles River Laboratories, Wilmington, MA). The animal legs were then flexed multiple times to distribute the injected solutes in the articular knee joint space. The rats were sacrificed 24 h after the intra-articular injection and the following knee tissues were collected: articular cartilage was scraped from the femoral condyle (FC), tibial plateau (TC), and patella (PC) using a scalpel; menisci (M); anterior and posterior cruciate ligaments (ACL and PCL); patellar tendons (PT) and quadriceps tendon (QT); and fat pad (FP). The weight of the harvested tissues was recorded, and tissue hydration was maintained throughout the experiments. We used N=6 joints per treatment condition including a saline control, for a total of 9 rats.

2.4.1. Confocal microscopy for rat tissue—Tissue samples extracted from the rat knee joints injected with saline, CPC +14A, and CPC +14N were imaged using Zeiss LSM 800 inverted confocal microscope at 10X magnification. Z stack of images along the tissue surface in X-Y plane was taken and processed using ImageJ to reconstruct the X-Z cross-section to evaluate the depth of penetration for each solute.

2.4.2. Quantitative measurement of CPC uptake in knee joint tissues—After imaging, the joint tissue samples were digested using Proteinase-K solution in 1 M Tris pH 8 for 48 h at 57°C to quantify the amount of CPC uptake by the tissues. The fluorescence of the digested samples was measured using a microplate reader (Synergy H1, Biotek). A standard curve of CPC in Proteinase-K in Tris buffer was used to convert the measured fluorescence values to moles of CPCs present in tissues, which was then normalized by the tissue wet weight.

2.5. Statistical analysis

All the data presented here is shown as Mean \pm Standard Deviation. At least, $n = 6$ cartilage explants per treatment condition were used for all *in-vitro* uptake and transport studies. Additionally, experiments were repeated using explants from at least 3 animals demonstrating consistent results. For microscale thermophoresis, $n = 3$ independent runs were performed for each target-ligand binding affinity measurement. K_d is reported as the Mean \pm Standard Deviation from all the runs. For *in vivo* intra-articular biodistribution rat studies, $N = 6$ joints/treatment were used, and CPC uptake data is reported as Mean \pm Standard Deviation for each tissue. For confocal microscopy, representative images are shown for each condition. A general linear mixed-effects model with animal as a random variable was used that showed no effect of animals, followed by Tukey's Honestly Significant Difference (Tukey's HSD) test to compare multiple treatment conditions. $P < 0.05$ was considered statistically significantly different.

3. Results

The GAG content of procured bovine SF was measured to be 103.6 ± 11.8 $\mu\text{g/mL}$, which falls within the range of severe OA stage [30]. Based on prior literature on human and animal SF, the following GAG concentration range is associated with OA severity: Normal SF < 25 $\mu\text{g/mL}$ GAGs; Moderate OA SF < 90 $\mu\text{g/mL}$ GAGs; Late-stage OA > 90 $\mu\text{g/mL}$

GAGs) [31,32]. Therefore, bovine SF is referred to as late-stage OA SF and the simulated synthetic SF is referred to as healthy condition.

3.1. Hydrophilic CPC +14N exhibits higher intra-cartilage uptake in presence of healthy and arthritic SF compared to its hydrophobic counterpart CPC +14A

The equilibrium intra-cartilage uptake of hydrophilic CPC +14N and its hydrophobic counterpart CPC +14A was measured in PBS, Healthy, and OA SF. CPC +14A and CPC +14N had similar very high mean uptake ratios (R_U) in cartilage in presence of PBS (~350) owing to charge interactions, implying 350x higher concentration of CPCs was present inside cartilage compared to the surrounding bath at equilibration (Fig. 3Ai). This uptake, however, was reduced by 4.5x and 2.7x for CPC +14A and CPC +14N respectively in presence of Healthy SF owing to competitive binding interactions (Fig. 3Aii); it is critical to note that these CPCs still maintained a very high intra-cartilage uptake in presence of SF ($R_U = 80$ for CPC +14A and 120 for CPC +14N). Importantly, hydrophilic CPC +14N demonstrated 1.5x and 2x higher intra-cartilage uptake compared to its hydrophobic counterpart, CPC +14A, in presence of Healthy and OA SF respectively (Figs. 3Ai–iii), highlighting the dominant role of hydrophobic interactions in causing competitive binding of CPCs within the SF. R+14, which has no hydrophilic or hydrophobic spacers, was used as a control and exhibited similar uptakes as CPC +14N in PBS and Healthy SF. In OA bovine SF, its uptake was measured to be 2x higher than CPC +14N potentially owing to its greater hydrophilic property. As expected, all CPC configurations had lower uptake in arthritic SF compared to healthy SF due to the presence of degraded GAG chains released from cartilage. Nevertheless, a high equilibrium intra-cartilage uptake of 15–20x for CPC +14N and R+14 in presence of OA SF highlights their potential in targeting cartilage at later OA stages.

3.2. Hydrophobic interactions play a more significant role than charge effects on the binding of cationic peptides within SF

In presence of physiological concentrations of negatively charged SF constituents HA and BSA, no significant difference in intra-cartilage uptake for CPC +14A and CPC +14N was observed (Fig. 3B, C). R+14 uptake dropped by more than half compared to the other two configurations in presence of HA, potentially owing to strong electrostatic binding interactions with HA due to its higher cationic charge density along the peptide length. However, in presence of hydrophobic γ -globulin, hydrophilic CPC +14N performed better as it exhibited 2.8x higher uptake compared to its hydrophobic counterpart (Fig. 3D). Similarly, CPC +14N exhibited higher uptake than CPC +14A in presence of phospholipids (DLPC) (Fig. 3E). In summary, the results suggest that the presence of hydrophobic alanine spacers increases CPC binding within SF especially to globulins while hydrophilic CPCs with asparagine spacers demonstrate greater cartilage targeting.

These findings were also corroborated by thermophoresis. Since Chondroitin sulfate-GAG (CS-GAG) is the most prevalent form of GAG in cartilage matrix [1,3], we measured its relative binding affinities with CPC +14A and +14N. Both CPCs demonstrated a very strong binding affinity towards CS-GAG (K_d of 526.5 ± 59 nM for CPC +14A and K_d of 626.1 ± 87 nM for CPC +14N, Fig. 4A). Also, both CPCs bound cooperatively with CS ($n = 3.9$ and

$n = 1.6$ for CPC +14A and +14N, respectively) potentially due to the effects of short-range hydrogen bonds that can synergistically stabilize charge-based binding [1,3]. This can be attributed partly to the presence of guanidinium head-groups on arginine that can form stable short-range hydrogen bonds with sulfated GAGs [33,34]. Additionally, guanidinium cations can form thermodynamically stable (weakly) like-charge pairs that can facilitate multiple of these peptides to come together by overcoming coulombic repulsions and bind more strongly to the same ligand site [35]. Finally, the hydrophobic CPC +14A showed a higher degree of cooperative binding potentially due to the presence of auxiliary hydrophobic interactions provided by the alanine spacers, which further stabilized its binding with CS-GAG.

In contrast, both CPCs remained completely unbound when titrated with HA as the ligand (Fig. 4B), with concentrations as high as the physiological concentration in SF (up to 2 μM). Further increase in HA concentration was limited by its solubility and the formation of a gel-like solution. On the other hand, at the same CS concentration, both CPCs were completely bound by the ligand, as discussed above. These results further confirm that electrostatic interactions are not the dominant cause of competitive binding for CPCs within SF. The K_d of γ -Globulin binding interaction with CPC +14A was 1.8x lower compared to that of hydrophilic CPC +14N ($143.0 \pm 30 \mu\text{M}$ for +14A vs $252.3 \pm 64 \mu\text{M}$ for +14N) demonstrating stronger binding affinity between the hydrophobic CPC and γ -Globulin (Fig. 4C). Both CPCs demonstrated negative cooperative binding with γ -Globulin ($n = 0.67$) likely owing to steric hindrance caused after saturation of the hydrophobic patch on globulin structure following initial binding of CPCs [36].

To further investigate the competitive effects of net charge vs. hydrophobicity on binding within the SF and cartilage targeting, we next compared the transport of CPC +14A with a new sequence CPC +8A, where we replaced 6 arginine residues with alanine thereby decreasing the net charge from +14 to +8 while nearly doubling the hydrophobicity (Table 2). Decreasing the net charge of CPC significantly reduced the intra-cartilage uptake by 6x in PBS (Fig. 5A) and by 5x and 3.5x in healthy and OA SF, respectively (Fig. 5B). CPC +8A demonstrated almost 90x lower affinity towards CS-GAG compared to CPC +14A ($K_d = 44.2 \pm 2.8 \mu\text{M}$ for CPC +8A vs $K_d = 526.5 \pm 59 \text{ nM}$ for CPC +14A, Fig. 5C and Table 4) owing to reduced net charge. This further highlights the importance of engineering carriers with an optimal net positive charge for effective cartilage targeting and maximal uptake, depending on the tissue's net negative FCD. Additionally, CPC +14A reported stronger cooperative binding with CS-GAG compared to CPC +8A (Table 4) due to a greater number of arginine residues containing guanidinium that can form stable short-range bidentate H-bonds with sulfated GAGs and further stabilize CPC's charge-based binding [34]. In contrast, doubling the hydrophobic residues in CPC +8A resulted in similar binding affinities with hydrophobic γ -Globulin as that of CPC +14A (Fig. 5D, Table 4). Both CPC +14A and CPC +8A demonstrated non-cooperative binding with γ -Globulin (Table 4) likely due to saturation of hydrophobic pockets on γ -Globulin by CPCs making subsequent CPC binding difficult. These results confirm that hydrophobic interactions play a more significant role in the binding of cationic carriers within SF than charge interactions thereby validating the use of electrostatics for developing cartilage targeting therapies. Additionally, CPC +14A's stronger binding with intra-cartilage residing CS-GAG indicates that short-range

effects of H-bonds can synergistically stabilize intra-cartilage charge-based binding - a strategy that can be utilized for enhancing intra-cartilage residence time of hydrophilic cationic carriers.

3.3. While hydrophobic interactions compete for binding within SF, they can stabilize charge-based binding in cartilage

To study the competitive effects of charge and hydrophobicity, we used a charge dominant K-rich CPC with net charge +7 (AK)₇ and then added a hydrophilic tail (ANANAN, asparagine spaced with alanine; **CPC +N**) or a hydrophobic tail (AFAFAF, phenylalanine with alanine; **CPC +F**. See Table 2). The primary amine groups in lysine are only capable of forming long-range electrostatic bonds but unlike arginine lack the ability to form hydrogen interactions [35].

Hydrophobic interactions stabilize charge-based binding in

cartilage: Hydrophobic CPC +F resulted in significantly higher uptake in both healthy and 90% GAG-depleted cartilage and had greater retention when desorbed in 1x or 10x PBS compared to its hydrophilic counterpart CPC +N (Fig. 6A,B) [1]. Thermophoresis also confirmed stronger binding of CPC +F with CS-GAG vs. CPC +N (Fig. 6C,D, Table 5). Positive cooperativity ($n = 1.6$) was measured for CPC +F, implying that the presence of hydrophobic bonds synergizes with charge interactions to facilitate its binding with CS-GAG. On the other hand, $n = 0.8$ for CPC +N with CS implies anti-cooperativity i.e., once the CPC is bound, the coulombic repulsion due to the same charge prevents engagement of another CPC at the same site.

Hydrophobic interactions compete for binding within SF: In presence of both healthy and arthritic SF, the trends were reversed; hydrophobic CPC +F resulted in lower intra-cartilage uptake vs. its hydrophilic counterpart, CPC +N (Fig. 6E). As expected, both CPCs had lower intra-cartilage uptake in presence of OA SF due to competing interactions with the degraded GAG chains released from cartilage. Intra-cartilage uptake in presence of globulins was lower for CPC +F vs. CPC +N, reinforcing the stronger binding effects of hydrophobic interactions within SF (Fig. 6F).

Therefore, similar to H-bonds (as demonstrated in Section 3.3 using CPC +14A whose arginine can form stable H-bonds with CS-GAG), hydrophobic effects can synergistically stabilize intra-cartilage charge based binding of cationic carriers. However, since hydrophobic effects are dominant in SF and can competitively bind with cationic carriers, it is important to make them hydrophilic and rely on synergistic effects of H-bonds (and not hydrophobic effects) for stabilizing intra-cartilage charge-based binding and the residence time of cationic carriers. This can be achieved by preferring arginine instead of lysine residues in the sequence as while both residues are cationic and hydrophilic, the guanidinium in arginine is capable of forming stable short-range bidentate H-bonds with cartilage CS-GAG.

3.4. Hydrophilic CPC +14N confirmed higher accumulation in rat knee tissues compared to its hydrophobic counterpart CPC +14A post-IA injection

Confocal images of rat joint tissues harvested 24 h following IA administration of CPCs showed significantly higher fluorescence signal for CPC +14N through the full thickness of femoral, tibial, and patellar cartilage as well as in menisci compared to CPC +14A (Fig. 7A). CPC +14N measured 2.5–3.5x higher accumulation compared to +14A in cartilage tissues (Fig. 7B). A weak fluorescence signal for both CPCs was detected in other less GAG-rich tissues including quadriceps and patellar tendon, and the fat pad. CPC uptake correlated strongly and positively with the mean GAG content of each tissue type ($R^2 = 0.9$ for both CPCs, Fig. 7C) further highlighting the important role of electrostatic interactions in intra-tissue CPC transport and retention. CPC +14N accumulated in the highest concentrations in the femoral cartilage which also had the highest GAG content (Table 6) followed by that in the tibial and patellar cartilage. Of note, no fluorescence was detected for the injected free dye at the same concentration at 24 h (data not shown).

4. Discussion

The work demonstrates that hydrophobic interactions play a more significant role than electrostatic interactions in the binding of cationic carriers within the synovial fluid (SF), which is rich in hydrophobic globulins and has about 20x lower negative fixed charge density (FCD) than cartilage (–170 mM in cartilage vs –8.8 mM in SF) [3]. This is an important finding as the use of cationic carriers for targeted drug delivery to negatively charged cartilage tissue has been contended to have limitations due to expected competitive binding with the anionic synovial fluid [18]. We used a previously designed arginine-rich cationic peptide carrier with a net charge of +14 containing non-polar alanine residues as spacers (CPC +14A), which was optimized for rapid full-thickness penetration into cartilage and greatest uptake and retention, and compared its transport with its hydrophilic counterpart, CPC +14N containing polar asparagine as spacers instead of alanine in presence of SF. The hydrophilic CPC +14N resulted in significantly greater intra-cartilage uptake in presence of both healthy and late-stage arthritic SF compared to CPC +14A (Fig. 3A). Interestingly, both CPCs maintained high intra-cartilage uptake without any significant difference in presence of physiological concentrations of individual negatively charged SF constituents HA and albumin (Fig. 3B–C). HA is the most abundant GAG in SF which is comprised of repeated negatively charged carboxylic groups, while albumin is the most abundant serum protein with an iso-electric point of 5 conferring a net negative charge at physiological pH [37]. However, in presence of hydrophobic globulins, CPC +14N had a 2.8x higher uptake in cartilage compared to its hydrophobic counterpart CPC +14A of the same charge and size (Fig. 3D). Both SF proteins globulins and albumin have hydrophobic amino acid residues, but the globulin's stable conformation exposes more hydrophobic patches compared to albumin conferring significantly higher surface net hydrophobicity [38,39]. While albumin's hydrophobicity did not affect CPC uptake, we identified globulin as the major protein constituent in SF that can form hydrophobic bonds with CPCs. Thermophoresis also confirmed stronger binding of CPC +14A with globulins (Fig. 4C). Consistent with our findings, a very low binding affinity between globulin and hydrophilic silanol-rich microspheres has been reported [40]. However, upon

modification of 9–43% of surface siloxane groups with hydrophobic trimethylchlorosilane groups, significant adsorption of γ -globulin on microspheres was reported [40].

Recently, Sharma and coworkers reported visible aggregation of amine-functionalized cationic polystyrene (PS) nanoparticles within SF [18], which was initially speculated to be electrostatic. However, no aggregation was observed when particles were incubated in HA implying that the interaction is not merely charge-based. Furthermore, didodecyldimethylammonium bromide (DMAB) nanoparticles consisting of quaternary ammonium with the same positive charge density as PS nanoparticles did not form aggregates within SF further suggesting that there are other dominant interactions. This makes sense as SF has significantly lower negative FCD than cartilage. Additionally, the binding affinity of CPCs with HA (which is the predominant GAG in SF) is significantly lower compared to that with CS-GAG, which is the most prevalent GAG in cartilage. Our thermophoresis measurements confirmed stronger binding of CPC +14A and CPC +14N with sulfated CS-GAG ($K_d = 526$ nM or 626 nM, respectively) while CPCs remained completely unbound when titrated with HA up to physiological concentrations (Fig. 4A, B). Similar differences between the binding affinity of viruses with sulfated and non-sulfated GAGs have been reported in the literature [41]. Viruses attach to the cell surface through electrostatic interactions between arginine residues in viral particles and proteoglycans like heparin sulfate in the cell membrane, which act as initial docking sites [42]. Similarly, significant binding of human cytomegalovirus (HCMV) with heparin sulfate has been reported while negligible binding with non-sulfated HA was observed [41].

The second major finding we report is that while hydrophobic effects compete for binding in the SF, they can *synergistically stabilize charge-based binding* within cartilage. To delineate this, we used lysine-rich CPCs instead of arginine. Unlike arginine which can form stable short-range H-bonds with GAGs, the primary amine in lysine can only form long-range electrostatic bonds [35,43]. A hydrophilic (CPC +N) or a hydrophobic tail (CPC +F) was added making them controlled sequences for investigating competitive vs. synergistic effects of charge and hydrophobic interactions. Consistent with our previous findings, hydrophilic CPC +N had greater intra-cartilage uptake than +F in presence of healthy or arthritic SF or globulins (Fig. 6E, F), confirming competing effects of hydrophobicity in SF. The hydrophobic CPC +F, however, had significantly greater intra-cartilage uptake and retention in both normal and GAG-depleted late-stage arthritic cartilage explants (Fig. 6B), which was also confirmed by MST that measured positive cooperativity ($n = 1.6$) for binding between +F and CS-GAG meaning hydrophobic effects can synergistically stabilize charge effects. On the other hand, negative cooperativity ($n = 0.8$) for +N and CS-GAG (Fig. 6C, D, Table 5) implies coulombic repulsion between CPCs due to the same charge, which is consistent with previous reports on the binding affinity between polylysine and lipid bilayer [43].

However, since hydrophobic effects are dominant in SF and can competitively bind with cationic carriers, it is important to make them hydrophilic and rely on synergistic effects of other effects like H-bonds (and not hydrophobic effects) for stabilizing intra-cartilage charge-based binding and the residence time of cationic carriers. This can be achieved by preferring arginine instead of lysine residues in the carrier sequence as while both residues are cationic and hydrophilic, the guanidinium in arginine is capable of forming

stable short-range bidentate H-bonds with cartilage CS-GAG [43]. This is supported by our Fig. 5 data which reports stronger cooperative binding of CPC +14A with CS-GAG compared to CPC +8A (Table 4) owing to a greater number of arginine residues. Therefore, a rational strategy for designing cationic carriers for targeting negatively charged tissues like cartilage in its native joint environment is to (1) make them hydrophilic to minimize their binding with the surrounding synovial fluid and (2) to rely on short-range H-bonds (e.g., by incorporating arginine) for enhancing intra-cartilage residence time. This is especially relevant when designing carriers for targeting arthritic cartilage with diminished FCD due to GAG degradation.

As IA administration is the primary route for drug delivery to the joint, drug delivery vehicles first come in contact with SF before diffusing into cartilage. However, only a few studies have investigated the interactions of nanoparticles with SF and considered its implications on cartilage targeting strategies [18,44,45]. Recently, it was shown that cationic PLGA particles underwent complete charge reversal following incubation in SF (+24.6 mV to -10.9 mV; hydrodynamic diameter increased from 261.5 nm to 300.6 nm) [18]. This masking of positive charge was attributed to adsorption of SF constituents on nanoparticle surface and formation of protein coronas [44,45]. The size and shape of nanoparticles are known factors to impact protein binding and the extent of the formation of protein coronas [46]. Naturally, smaller nanoparticles with lower surface area bind lower amounts of protein on their surface [46]. For example, 2 nm gold nanoparticles were shown not to form protein coronas while larger particles with the same surface chemistry formed conventional coronas [47]. The small size of CPCs (~3-4 kDa) makes them unlikely candidates for forming protein coronas. While the *ex vivo* transport models used here help investigate the mechanistic effects of electrostatic and hydrophobic interactions on the binding of CPCs within SF, they do not incorporate the effect of rapid SF turnover and compression-induced convective flow. SF proteins turnover rapidly every 1 h while hyaluronic acid has a slower turnover rate of around 13 h in healthy joints [48]. Therefore, we investigated the biodistribution of hydrophobic CPC +14A and hydrophilic CPC +14N in rat knees following their IA administration. Consistent with our *ex vivo* findings, CPC +14N had significantly greater accumulation than its hydrophobic counterpart CPC +14A and was present through the full thickness of femoral, tibial, patellar cartilage, and menisci (Fig. 7) at 24 h.

In summary, the rapid and high intra-cartilage uptake, as well as full tissue thickness penetration of CPC +14N, can be attributed to its optimal net cationic charge while it is its hydrophilic property that minimizes its binding within the synovial fluid, making it an ideal candidate for drug delivery to cartilage. The presence of arginine residues stabilizes the intra-cartilage charge-based binding via short-range H-bonds. CPC +14N, therefore, can also be effective in targeting arthritic cartilage with diminished negative FCD.

5. Conclusions

This work demonstrates that hydrophobic interactions and not charge interactions are the dominant cause of the binding of cationic carriers in synovial fluid. Hydrophobic interactions can also synergistically stabilize long-range electrostatic binding in cartilage – a mechanism that can be used for enhancing the targeting and residence time of cationic

carriers within arthritic cartilage with reduced negative FCD. However, since hydrophobic effects can cause the binding of carriers within the synovial fluid, short-range effects like H-bonds can be utilized. It is, therefore, proposed to make cationic carriers hydrophilic and prefer arginine over lysine in the sequence. Finally, the cartilage-synovial fluid model used here provides an excellent model of a complex negatively charged environment and allows us to generalize these findings to other tissue systems of varying FCD and develop targeted therapies for another complex negatively charged environment with varying net FCD.

Acknowledgements

This work was supported by the National Science Foundation (NSF) CAREER AWARD 2141841 and [National Institutes of Health](#) (NIH) R01AR075121.

References

- [1]. Vedadghavami A, Wagner EK, Mehta S, He T, Zhang C, Bajpayee AG, Cartilage penetrating cationic peptide carriers for applications in drug delivery to avascular negatively charged tissues, *Acta Biomater.* 93 (2019) 258–269, doi:10.1016/j.actbio.2018.12.004. [PubMed: 30529083]
- [2]. Bajpayee AG, Scheu M, Grodzinsky AJ, Porter RM, Electrostatic interactions enable rapid penetration, enhanced uptake and retention of intra-articular injected avidin in rat knee joints, *J. Orthop. Res* 32 (2014) 1044–1051, doi:10.1002/jor.22630. [PubMed: 24753019]
- [3]. Vedadghavami A, Zhang C, Bajpayee AG, Overcoming negatively charged tissue barriers: drug delivery using cationic peptides and proteins, *Nano Today* 34 (2020) 100898, doi:10.1016/j.nantod.2020.100898. [PubMed: 32802145]
- [4]. Wagner EK, Vedadghavami A, Jacobsen TD, Goel SA, Chahine NO, Bajpayee AG, Avidin grafted dextran nanostructure enables a month-long intra-discal retention, *Sci. Rep* 10 (2020) 1–14 2020 101, doi:10.1038/s41598-020-68351-1. [PubMed: 31913322]
- [5]. Bajpayee AG, Grodzinsky AJ, Cartilage-targeting drug delivery: can electrostatic interactions help? *Nat. Rev. Rheumatol* 13 (2017) 183–193, doi:10.1038/nrrheum.2016.210. [PubMed: 28202920]
- [6]. Graham BT, Moore AC, Burris DL, Price C, Sliding enhances fluid and solute transport into buried articular cartilage contacts, *Osteoarthr. Cartil* 25 (2017) 2100–2107, doi:10.1016/J.JOCA.2017.08.014.
- [7]. Ngo L, Knothe Tate ML, Osteoarthritis: new strategies for transport and drug delivery across length scales, *ACS Biomater. Sci. Eng* 6 (2020) 6009–6020, doi:10.1021/ACSBIOMATERIALS.0C01081/ASSET/IMAGES/MEDIUM/AB0C01081_0005.GIF. [PubMed: 33449636]
- [8]. Mehta S, He T, Bajpayee AG, Recent advances in targeted drug delivery for treatment of osteoarthritis, *Curr. Opin. Rheumatol* 33 (2021) 94–109, doi:10.1097/BOR.0000000000000761. [PubMed: 33229973]
- [9]. Mehta S, Akhtar S, Porter RM, Önnarfjord P, Bajpayee AG, Interleukin-1 receptor antagonist (IL-1Ra) is more effective in suppressing cytokine-induced catabolism in cartilage-synovium co-culture than in cartilage monoculture, *Arthritis Res. Ther* 21 (2019) 238, doi:10.1186/s13075-019-2003-y. [PubMed: 31722745]
- [10]. Young CC, Vedadghavami A, Bajpayee AG, Bioelectricity for drug delivery: the promise of cationic therapeutics, *Bioelectricity* 2 (2020) 68–81, doi:10.1089/bioe.2020.0012. [PubMed: 32803148]
- [11]. Bajpayee AG, Quadir MA, Hammond PT, Grodzinsky AJ, Charge based intra-cartilage delivery of single dose dexamethasone using Avidin nano-carriers suppresses cytokine-induced catabolism long term, *Osteoarthr. Cartil* 24 (2016) 71–81, doi:10.1016/j.joca.2015.07.010.
- [12]. Bajpayee AG, Wong CR, Bawendi MG, Frank EH, Grodzinsky AJ, Avidin as a model for charge driven transport into cartilage and drug delivery for treating early stage post-traumatic

osteoarthritis, *Biomaterials* 35 (2014) 538–549, doi:10.1016/j.biomaterials.2013.09.091. [PubMed: 24120044]

- [13]. He T, Zhang C, Vedadghavami A, Mehta S, Clark HA, Porter RM, Bajpayee AG, Multi-arm Avidin nano-construct for intra-cartilage delivery of small molecule drugs, *J. Control. Release* 318 (2020) 109–123, doi:10.1016/j.jconrel.2019.12.020. [PubMed: 31843642]
- [14]. Zhang C, He T, Vedadghavami A, Bajpayee AG, Avidin-biotin technology to synthesize multi-arm nano-construct for drug delivery, *MethodsX* 7 (2020) 100882, doi:10.1016/J.MEX.2020.100882. [PubMed: 32405463]
- [15]. Bajpayee AG, Scheu M, Grodzinsky AJ, Porter RM, A rabbit model demonstrates the influence of cartilage thickness on intra-articular drug delivery and retention within cartilage, *J. Orthop. Res* 33 (2015) 660–667, doi:10.1002/jor.22841. [PubMed: 25627105]
- [16]. Warren MR, Bajpayee AG, Modeling electrostatic charge shielding induced by cationic drug carriers in articular cartilage using donnan osmotic theory, *Bioelectricity* (2021), doi:10.1089/bioe.2021.0026.
- [17]. He T, Shaw I, Vedadghavami A, Bajpayee AG, Single-dose intra-cartilage delivery of kartogenin using a cationic multi-arm avidin nanocarrier suppresses cytokine-induced osteoarthritis-related catabolism, *Cartilage* 13 (2022), doi:10.1177/19476035221093072.
- [18]. Brown S, Pistiner J, Adjei IM, Sharma B, Nanoparticle properties for delivery to cartilage: the implications of disease state, synovial fluid, and off-target uptake, *Mol. Pharm* 16 (2019) 469–479, doi:10.1021/acs.molpharmaceut.7b00484. [PubMed: 28669194]
- [19]. Tamer TM, Hyaluronan and synovial joint: function, distribution and healing, *Interdiscip. Toxicol* 6 (2013) 111, doi:10.2478/INTOX-2013-0019. [PubMed: 24678248]
- [20]. Hui AY, McCarty WJ, Masuda K, Firestein GS, Sah RL, A systems biology approach to synovial joint lubrication in health, injury, and disease, *Wiley Interdiscip. Rev. Syst. Biol. Med* 4 (2012) 15, doi:10.1002/WSBM.157.
- [21]. Kusayama Y, Akamatsu Y, Kumagai K, Kobayashi H, Aratake M, Saito T, Changes in synovial fluid biomarkers and clinical efficacy of intra-articular injections of hyaluronic acid for patients with knee osteoarthritis, *J. Exp. Orthop* 1 (2014) 1–9, doi:10.1186/S40634-014-0016-7. [PubMed: 26914746]
- [22]. Kyte J, Doolittle RF, A simple method for displaying the hydropathic character of a protein, *J. Mol. Biol* 157 (1982) 105–132, doi:10.1016/0022-2836(82)90515-0. [PubMed: 7108955]
- [23]. Coulson-Thomas V, Gesteira T, Dimethylmethylene blue assay (DMMB), *Bio-Protocol* 4 (2016), doi:10.21769/bioprotoc.1236.
- [24]. Bortel EL, Charbonnier B, Heuberger R, Development of a synthetic synovial fluid for tribological testing, *Lubricants* 3 (2015) 664–686, doi:10.3390/lubricants3040664.
- [25]. Stark N, S Streckenbach M, Gilchrist S, Schwenke T, Thomas B, Synthetic synovial fluid compositions and methods for making the same (Patent No. US20120186356A1) (2012), <https://patents.google.com/patent/US20120186356A1/en>
- [26]. Fardale RW, Sayers CA, Barrett AJ, A direct spectrophotometric microassay for sulfated glycosaminoglycans in cartilage cultures, *Connect. Tissue Res* 9 (1982) 247–248, doi:10.3109/03008208209160269. [PubMed: 6215207]
- [27]. Vedadghavami A, Mehta S, Bajpayee AG, Characterization of intra-cartilage transport properties of cationic peptide carriers, *J. Vis. Exp* 2020 (2020) 1–22, doi:10.3791/61340.
- [28]. Jerabek-Willemsen M, André T, Wanner R, Roth HM, Duhr S, Baaske PD Breitsprecher, MicroScale Thermophoresis: interaction analysis and beyond, *J. Mol. Struct* 1077 (2014) 101–113, doi:10.1016/J.MOLSTRUC.2014.03.009.
- [29]. Stefan MI, Le Novère N, Cooperative binding, *PLOS Comput. Biol.* 9 (2013), doi:10.1371/journal.pcbi.1003106.
- [30]. Mattiello-Rosa SMG, Cintra Neto PFA, Lima GEG, Pinto KNZ, Cohen M, Pimentel DR, Glycosaminoglycan loss from cartilage after anterior cruciate ligament rupture: influence of time since rupture and chondral injury, *Braz. J. Phys. Ther* 12 (2008) 64–69, doi:10.1590/S1413-35552008000100012.
- [31]. Palmer JL, Bertone AL, McClain H, Assessment of glycosaminoglycan concentration in equine synovial fluid as a marker of joint disease, *Can. J. Vet. Res* 59 (1995) 205. [PubMed: 8521354]

- [32]. Kulkarni P, Deshpande S, Koppikar S, Patil S, Ingale D, Harsulkar A, Glycosaminoglycan measured from synovial fluid serves as a useful indicator for progression of Osteoarthritis and complements Kellgren–Lawrence Score, *BBA Clin.* 6 (2016) 1, doi:10.1016/J.BBACLI.2016.05.002. [PubMed: 27331021]
- [33]. Rothbard JB, Jessop TC, Lewis RS, Murray BA, Wender PA, Role of membrane potential and hydrogen bonding in the mechanism of translocation of guanidinium-rich peptides into cells, *J. Am. Chem. Soc.* 126 (2004) 9506–9507, doi:10.1021/JA0482536. [PubMed: 15291531]
- [34]. Åmand HL, Rydberg HA, Fornander LH, Lincoln P, Nordén B, Esbjörner EK, Cell surface binding and uptake of arginine- and lysine-rich penetratin peptides in absence and presence of proteoglycans, *Biochim. Biophys. Acta* 1818 (2012) 2669–2678, doi:10.1016/J.BBAMEM.2012.06.006. [PubMed: 22705501]
- [35]. Vazdar M, Heyda J, Mason PE, Tesei G, Allolio C, Lund M, Jungwirth P, Arginine “magic”: guanidinium like-charge ion pairing from aqueous salts to cell penetrating peptides, *Acc. Chem. Res* 51 (2018) 1455–1464, doi:10.1021/acs.accounts.8b00098. [PubMed: 29799185]
- [36]. Janeway C Jr, Travers P, et al. , The interaction of the antibody molecule with specific antigen, *Immunobiology: The Immune System in Health and Disease*, Garland Science, 2001 <https://www.ncbi.nlm.nih.gov/books/NBK27160/>.
- [37]. Wiig H, Kolmannskog O, Tenstad O, Bert JL, Effect of charge on interstitial distribution of albumin in rat dermis *in vitro*, *J. Physiol* 550 (2003) 505, doi:10.1113/JPHYSIOL.2003.042713. [PubMed: 12766239]
- [38]. Sugimura Y, Fukunaga K, Matsuno T, Nakao K, Goto M, Nakashio F, A study on the surface hydrophobicity of lipases, *Biochem. Eng. J* 5 (2000) 123–128, doi:10.1016/S1369-703X(99)00072-8. [PubMed: 10817817]
- [39]. Nwachukwu ID, Aluko RE, Physicochemical and emulsification properties of flaxseed (*Linum usitatissimum*) albumin and globulin fractions, *Food Chem.* 255 (2018) 216–225, doi:10.1016/J.FOODCHEM.2018.02.068. [PubMed: 29571469]
- [40]. Mizerska U, Fortuniak W, Pospiech P, Sobczak A, Chojnowski J, Slomkowski S, Hydrophilic–hydrophobic properties of SiOH-loaded and modified polysiloxane microspheres and their interaction with γ -globulin, *Polym. Adv. Technol* 26 (2015) 855–864, doi:10.1002/PAT.3494.
- [41]. Mitra D, Hasan MH, Bates JT, Bierdeman MA, Ederer DR, Parmar RC, Fassero LA, Liang Q, Qiu H, Tiwari V, Zhang F, Linhardt RJ, Sharp JS, Wang L, Tandon R, The degree of polymerization and sulfation patterns in heparan sulfate are critical determinants of cytomegalovirus entry into host cells, *PLoS Pathog.* 17 (2021) e1009803, doi:10.1371/JOURNAL.PPAT.1009803. [PubMed: 34352038]
- [42]. Villanueva RA, Rouillé Y, Dubuisson J, Interactions between virus proteins and host cell membranes during the viral life cycle, *Int. Rev. Cytol* 245 (2005) 171–244, doi:10.1016/S0074-7696(05)45006-8. [PubMed: 16125548]
- [43]. Robison AD, Sun S, Poyton MF, Johnson GA, Pellois JP, Jungwirth P, Vazdar M, Cremer PS, Polyarginine interacts more strongly and cooperatively than polylysine with phospholipid bilayers, *J. Phys. Chem. B* 120 (2016) 9287–9296, doi:10.1021/acs.jpcc.6b05604. [PubMed: 27571288]
- [44]. Kumar S, Sharma B, Leveraging electrostatic interactions for drug delivery to the joint, *Bioelectricity* 2 (2020) 82–100, doi:10.1089/BIOE.2020.0014. [PubMed: 32856016]
- [45]. Brown S, Kumar S, Sharma B, Intra-articular targeting of nanomaterials for the treatment of osteoarthritis, *Acta Biomater.* 93 (2019) 239–257, doi:10.1016/J.ACTBIO.2019.03.010. [PubMed: 30862551]
- [46]. Park SJ, Protein–nanoparticle interaction: corona formation and conformational changes in proteins on nanoparticles, *Int. J. Nanomed* 15 (2020) 5783, doi:10.2147/IJN.S254808.
- [47]. Boselli L, Polo E, Castagnola V, Dawson KA, Regimes of biomolecular ultrasmall nanoparticle interactions, *Angew. Chemie* 129 (2017) 4279–4282, doi:10.1002/ANGE.201700343.
- [48]. Goldring SR, Goldring MB, biology of the normal joint, *Kelley’s Textbook of Rheumatology*, W.B. Saunders, 2013 pp. 1–19.e6, doi:10.1016/b978-1-4377-1738-9.00001-3.

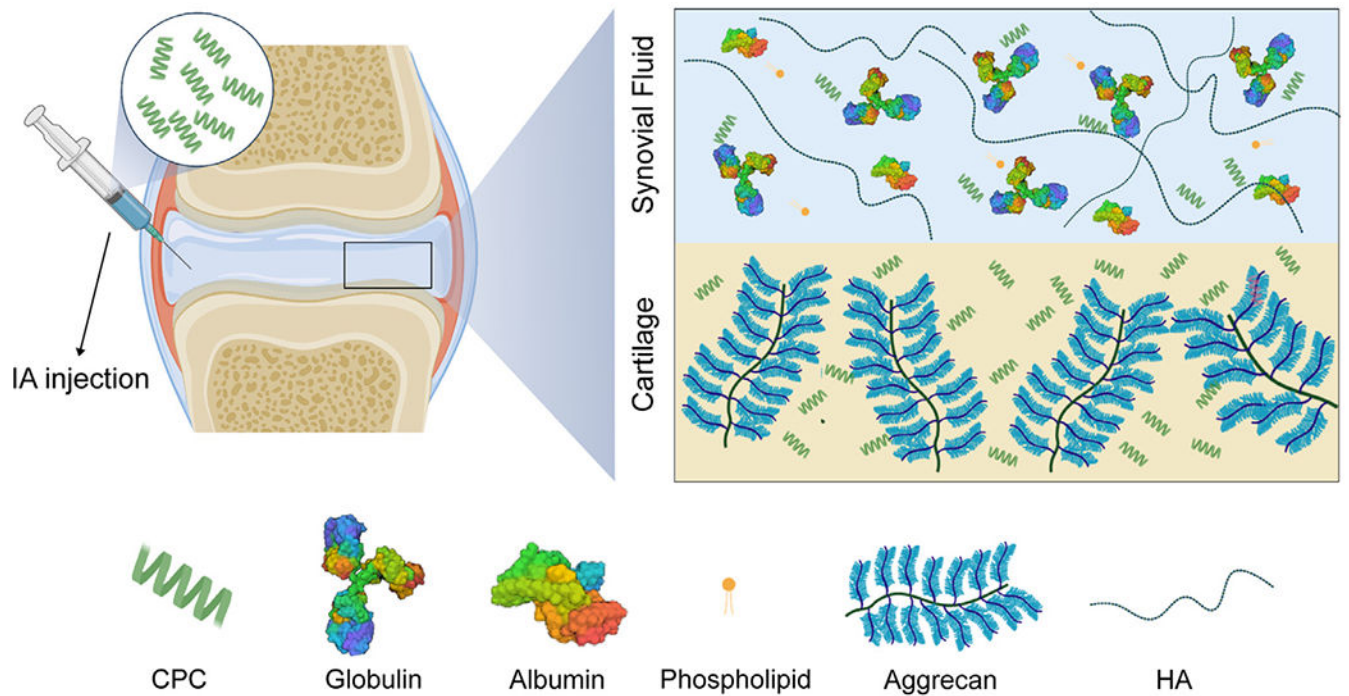


Fig. 1.

Charge interactions enable rapid and full depth penetration of CPCs into negatively charged cartilage. The synovial joint is filled with synovial fluid (SF), which is comprised of a high concentration of negatively charged constituents, hyaluronic acid (HA) and albumin, and hydrophobic immunoglobulins and phospholipids that may alter or hamper the cartilage targeting ability of intra-articularly administered therapeutics.

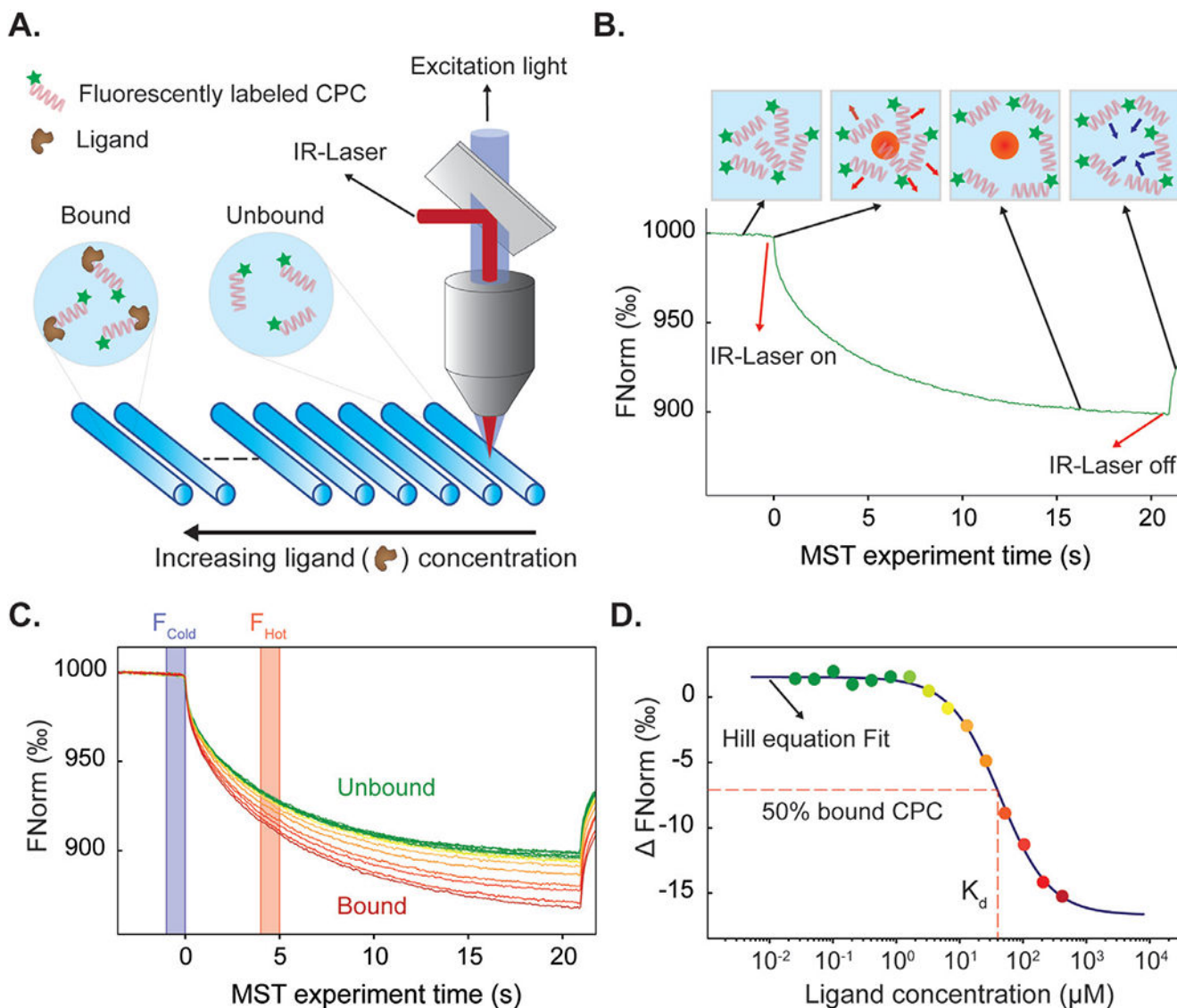
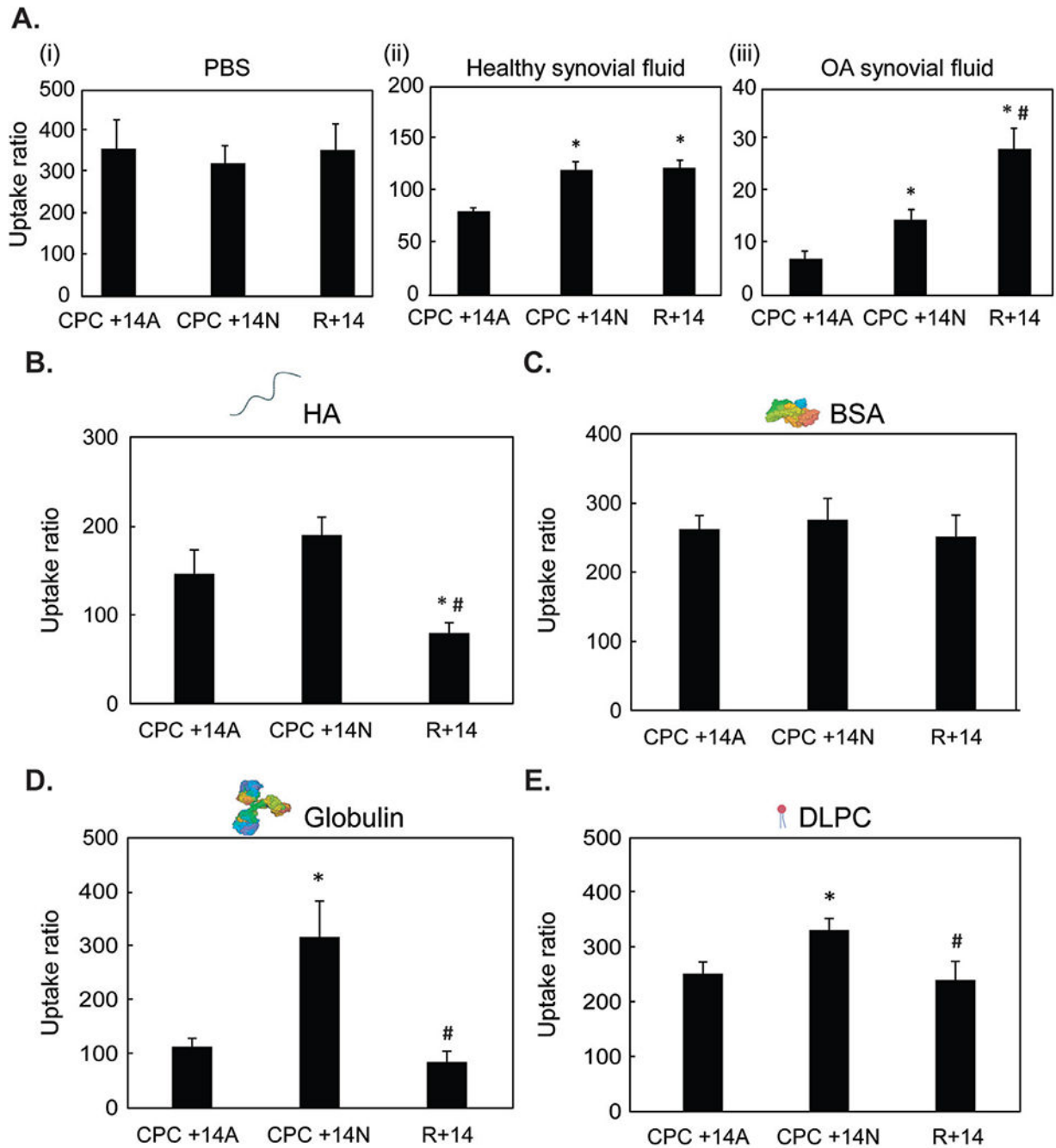


Fig. 2. Methodology for measuring binding affinity of CPCs with cartilage and SF constituents using microscale thermophoresis (MST). **A.** A fixed concentration of fluorescently labeled CPC is titrated with varying concentrations of a ligand molecule. CPCs are completely unbound in the highly dilute state while they are fully bound at high ligand concentrations. Samples are then loaded in capillary tubes and heated locally with an infrared (IR) laser to create a temperature fluorescence gradient. **B.** The normalized fluorescence (F_{Norm}) is recorded for 20 s to obtain an MST trace curve. **C.** The MST traces of all samples from varying concentrations of ligands are plotted over a span of 20 s. **D.** Dose-dependent binding of CPC with its ligand further alters the fluorescence, which is measured as MST and plotted vs the respective ligand concentration. Hill equation is fitted to extract K_d and Hill coefficient (n). $n > 1$ represents positive cooperative binding while $n < 1$ implies negative cooperative binding.

**Fig. 3.**

A. Intra-cartilage equilibrium uptake of CPC +14A, CPC +14N, and R+14 in (i) PBS, (ii) healthy synovial fluid, and (iii) OA synovial fluid, and in presence of the following individual SF constituents at physiological concentrations: **B.** HA, **C.** BSA, **D.** γ -Globulin and **E.** DLPC. * vs CPC +14A, # vs CPC +14N; $p < 0.05$.

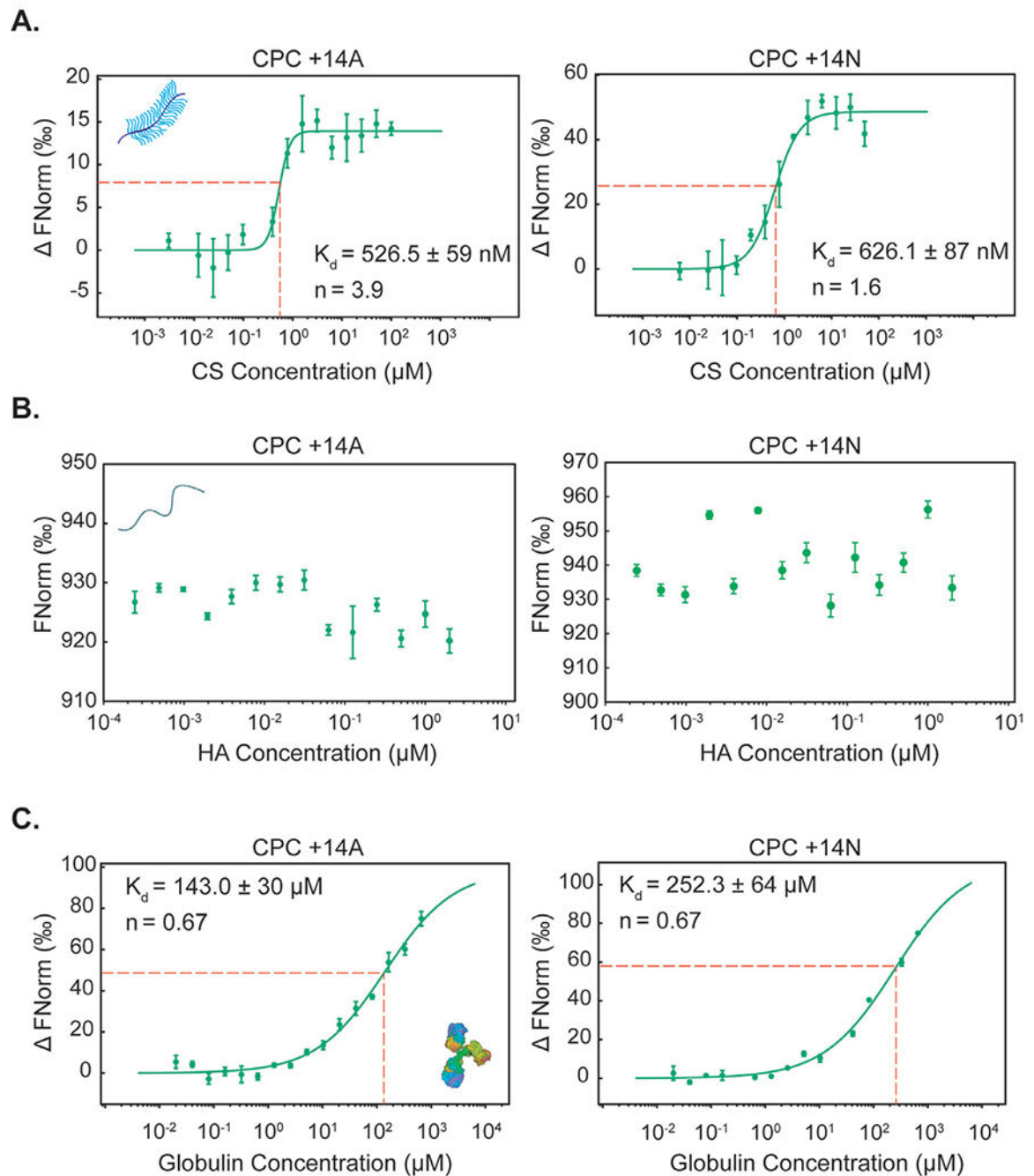


Fig. 4. Comparison between binding properties of CPC +14A and CPC +14N with the following ligands determined using MST: **A.** Chondroitin sulfate (CS), **B.** Hyaluronic acid (HA) **C.** γ -Globulin.

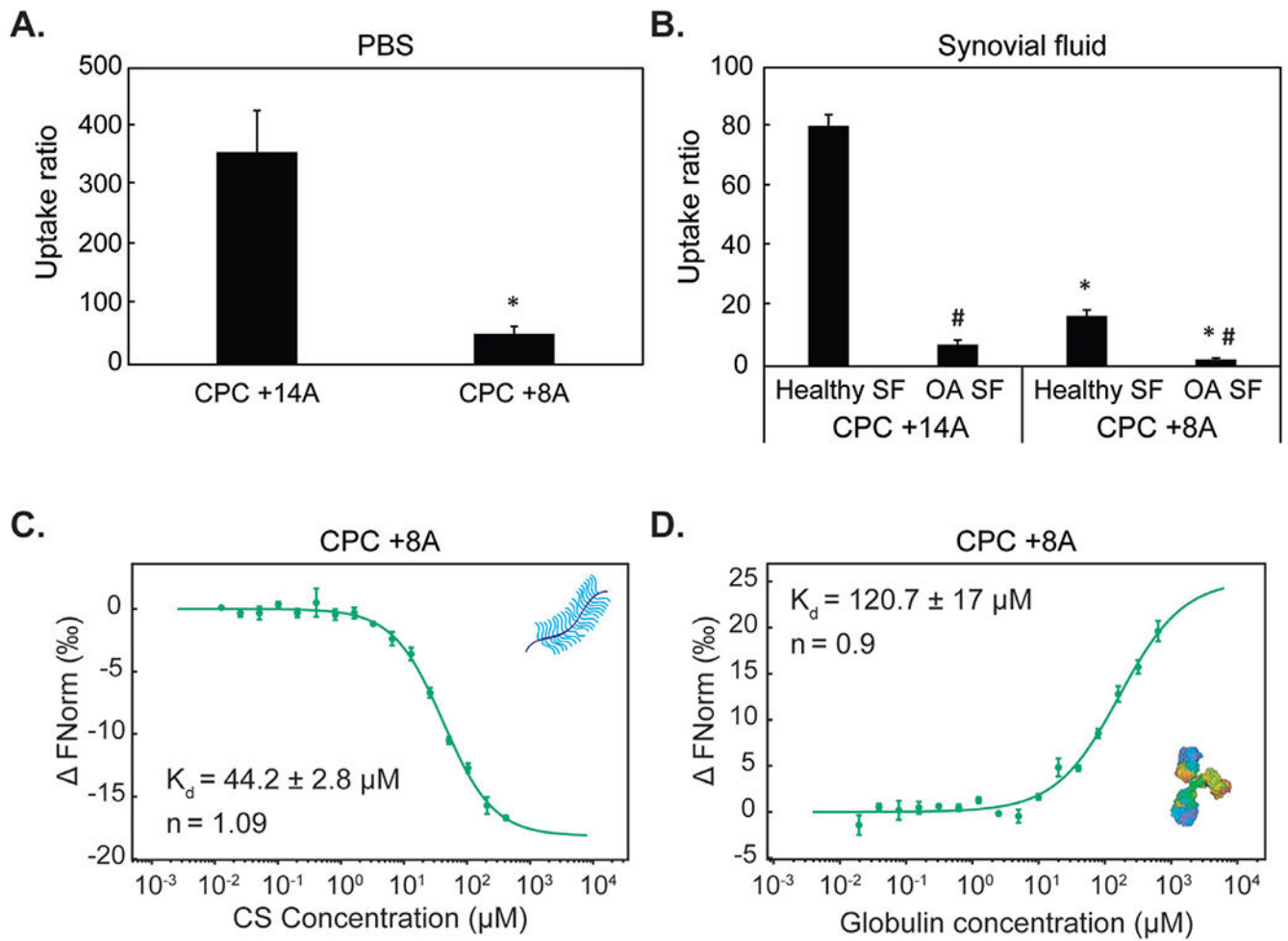
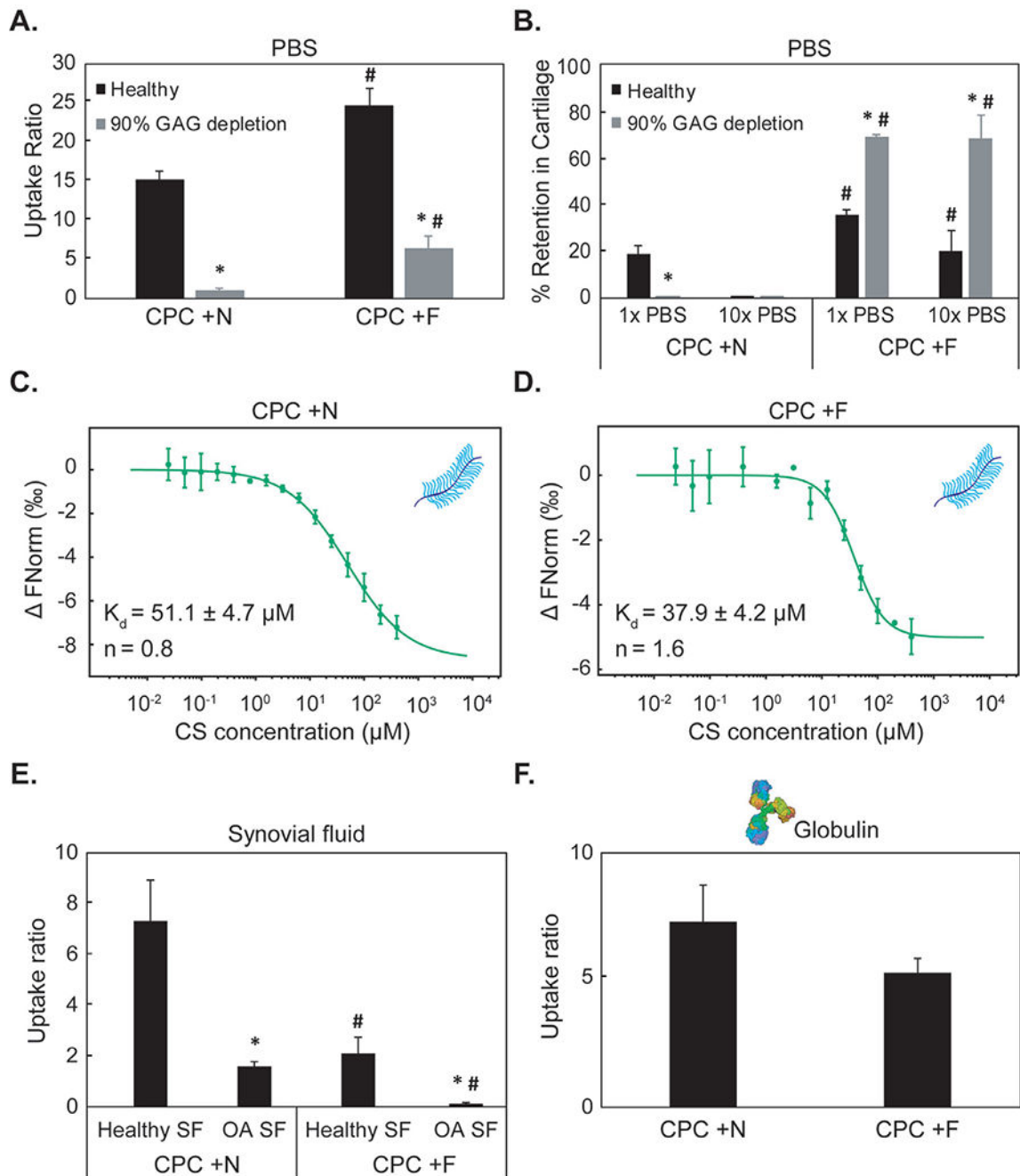


Fig. 5. Intra-cartilage equilibrium uptake of CPC +14A and CPC +8A in **A.** PBS and **B.** healthy and OA synovial fluid. * vs CPC +14A, # vs Healthy SF; $p < 0.05$. Dissociation constants (K_d) and cooperativity factors (n) are determined using MST for binding of CPC +8A with **C.** Chondroitin sulfate (CS) and **D.** γ -Globulin.

**Fig. 6.**

A. Comparison between equilibrium uptake of hydrophilic CPC +N and its hydrophobic counterpart CPC +F in healthy and 90% GAG depleted cartilage in PBS. **B.** % Intra-cartilage CPC retention following 24 h desorption in 1x and 10x PBS bath. Adapted with permission from [1]. Dissociation constants (K_d) and cooperativity factors (n) are determined using MST for binding between chondroitin sulfate (CS) and **C.** CPC +N or **D.** CPC +F. **E.** Intra-cartilage uptake of CPC +N and CPC +F equilibrated in γ -Globulin at physiological

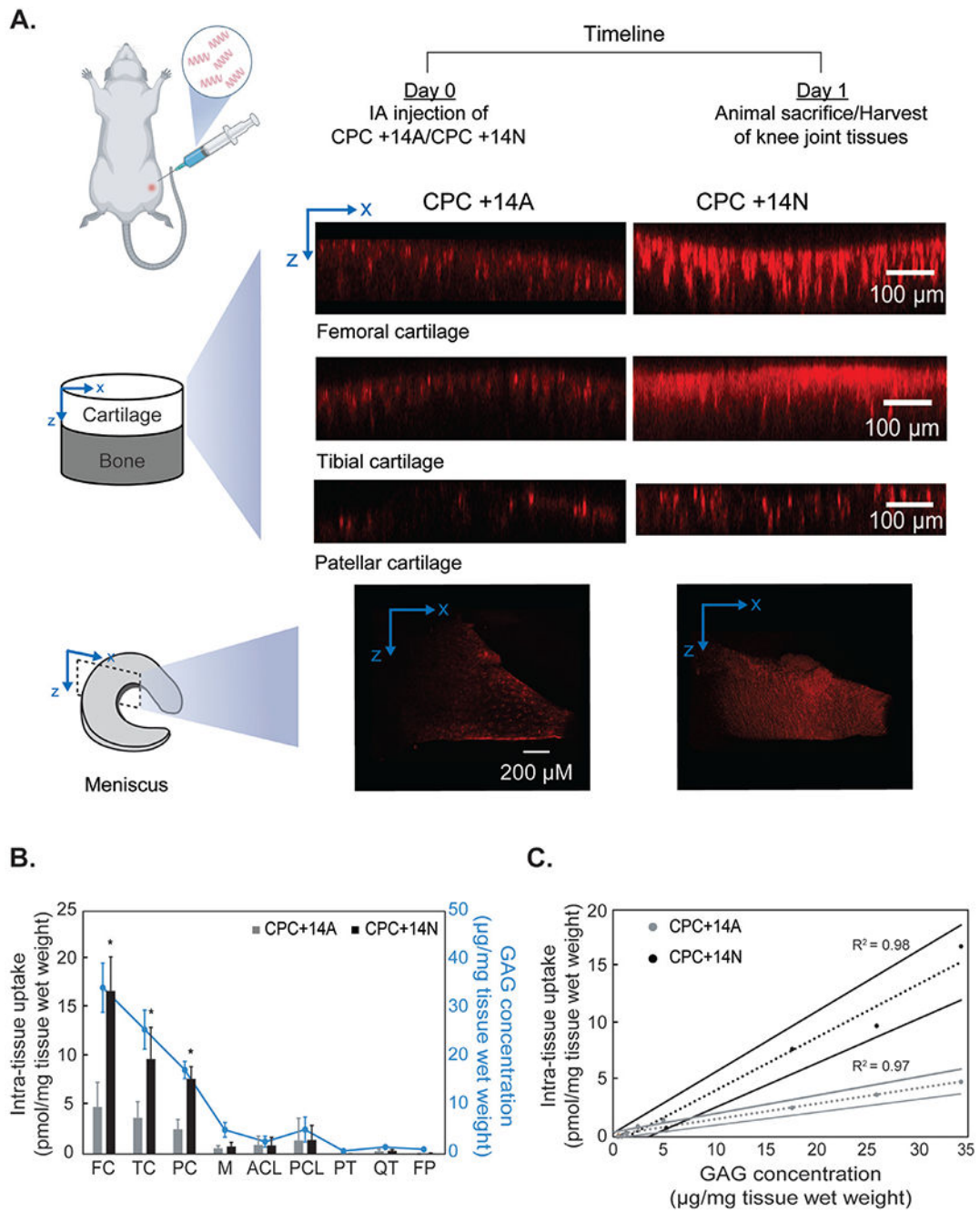
SF concentration **F**. Intra-cartilage uptake of CPC +N and CPC +F equilibrated in healthy and OA SF. * vs healthy, # vs corresponding condition in CPC +N; $p < 0.05$.

Author Manuscript

Author Manuscript

Author Manuscript

Author Manuscript

**Fig. 7.**

A. Confocal images showing distribution and depth of penetration of CPC +14A and CPC +14N in various rat knee tissues 24 h post-intra-articular injection. **B.** CPC uptake in different rat knee tissues 24 h after intra-articular injection. Data are shown as Mean \pm standard deviation. Tissue GAG concentration is shown in blue. **C.** Correlation between intra-tissue uptake of CPCs and GAG concentration is plotted. The dotted line is the linear least squared fit and solid lines show 95% confidence intervals (Femoral cartilage: FC;

Tibial cartilage: TC; Patellar cartilage: PC; Meniscus: M; Anterior crucial ligament: ACL;
Posterior crucial ligament: PCL; Patellar tendon: PT; Quadriceps tendon: QT; Fat pad: FP).

Author Manuscript

Author Manuscript

Author Manuscript

Author Manuscript

Table 1

Primary constituents of synovial fluid and cartilage matrix, their concentrations, and resulting net negative fixed charge density (FCD) y DMMB assay.

Synovial fluid constituents	Concentration (mg/ml)	FCD (mM)
HA	1–4 [19]	–8.8 [3]
Albumin	12 [20]	-
Globulin (β_1 , γ , α_1 & α_2)	1–3 (each) [20]	-
Phospholipid	0.1 [19]	-
Cartilage constituents	Concentration ($\mu\text{g}/\text{mg}$ wet tissue)	FCD (mM)
CS	30	–170 [3]

Author Manuscript

Author Manuscript

Author Manuscript

Author Manuscript

Table 2

Cationic Peptide Carriers (CPC): Sequence, net charge, and molecular weight.

CPC	CPC Sequence	Net charge (z)	MW (Da)	Property
CPC +14A	RRRR(AARRR) ₃ R	+14	2,990	Hydrophobic
CPC +14N	RRRR(NNRRR) ₃ R	+14	3,248	Hydrophilic
R+14	R ₁₄	+14	2,563	Hydrophilic
CPC +8A	(RRAAAA) ₃ RR	+8	2,479	Hydrophobic
CPC +N	(AK) ₇ ANANAN	+7	2,327	Hydrophilic
CPC +F	(AK) ₇ AFAFAF	+7	2,426	Hydrophobic

Author Manuscript

Author Manuscript

Author Manuscript

Author Manuscript

Table 3

Hydropathy scale of different amino acids with 4.5 being the most hydrophobic and -4.5 the most hydrophilic residue (Table adapted from [22]).

Residue	Hydropathy index
Ile	4.5
Val	4.2
Leu	3.8
Phe	2.8
Cys	2.5
Met	1.9
Ala	1.8
Gly	-0.4
Thr	-0.7
Ser	-0.8
Trp	-0.9
Tyr	-1.3
Pro	-1.6
His	-3.2
Glu	-3.5
Gln	-3.5
Asp	-3.5
Asn	-3.5
Lys	-3.9
Arg	-4.5

Author Manuscript

Author Manuscript

Author Manuscript

Author Manuscript

Table 4

Dissociation constant (K_d) and cooperativity factor (n) of binding interactions between CPC +8A and CPC +14A with CS-GAG and γ -Globulin determined using microscale thermophoresis.

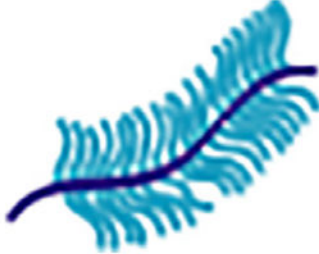
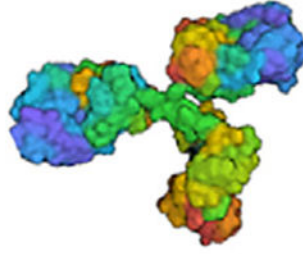

Ligand	CPC	K_d	n
	CPC +8A	$44.2 \pm 2.8 \mu M$	1.09
	CPC +14A	$526.5 \pm 59 nM$	3.9
	CPC +8A	$120.7 \pm 17 \mu M$	0.9
	CPC +14A	$143.0 \pm 30 \mu M$	0.67

Table 5

Dissociation constant (K_d) and cooperativity factor (n) of binding interactions between CPC +N and CPC +F with CS-GAG determined using microscale thermophoresis.

Ligand	CPC	K_d	n
	CPC +N	$51.1 \pm 4.7 \mu M$	0.8
	CPC +F	$37.9 \pm 4.2 \mu M$	1.6

Author Manuscript

Author Manuscript

Author Manuscript

Author Manuscript

Table 6

Mean GAG content of different rat tissues determined b.

Tissue	FC	TC	PC	M	ACL	PCL	PT	QT	FP
GAG content (µg/mg tissue wet weight)	34.3	26	17.7	5.2	2.4	4.9	0.5	1.3	0.9